Alexandre François, Nicolas Riesen, Kirsty Gardner, Tanya M. Monro, and Al Meldrum
Lasing of whispering gallery modes in optofluidic microcapillaries
Optics Express, 2016; 24(12):12466-12477

Lasing of whispering gallery modes in optofluidic microcapillaries

Alexandre François,[1,2,*] Nicolas Riesen,[1] Kirsty Gardner,[3] Tanya M. Monro,[1,2] and Al Meldrum[3]

[1]*The Institute for Photonics and Advanced Sensing (IPAS), School of Physical Sciences, The University of Adelaide, SA 5005, Adelaide, Australia*
[2]*University of South Australia, SA 5000, Adelaide, Australia*
[3]*Department of Physics, University of Alberta, Edmonton, AB, T6G2E1, Canada*
[*]*alexandre.francois@unisa.edu.au*

Abstract: This paper demonstrates lasing of the whispering gallery modes in polymer coated optofluidic capillaries and their application to refractive index sensing. The laser gain medium used here is fluorescent Nile Red dye, which is embedded inside the high refractive index polymer coating. We investigate the refractometric sensing properties of these devices for different coating thicknesses, revealing that the high Q factors required to achieve low lasing thresholds can only be realized for relatively thick polymer coatings (in this case ≥ 800 nm). Lasing capillaries therefore tend to have a lower refractive index sensitivity, compared to non-lasing capillaries which can have a thinner polymer coating, due to the stronger WGM confinement within the polymer layer. However we find that the large improvement in signal-to-noise ratio realized for lasing capillaries more than compensates for the decreased sensitivity and results in an order-of-magnitude improvement in the detection limit for refractive index sensing.

OCIS codes: (120.0280) Remote sensing and sensors; (140.33948) Microcavity devices; (140.3410) Laser resonators; (140.3560) Lasers, ring; (230.5750) Resonators; (310.6628) Subwavelength structures, nanostructures.

References and links

1. F. Vollmer, and S. Roy, "Optical resonator based biomolecular sensors and logic devices," J. Indian Inst. Sci. **92**, 233-251 (2012).
2. V. Lefevre-Seguin, "Whispering gallery mode lasers with doped silica microspheres," Opt. Mater. **11**, 153-165 (1999).
3. L. He, S. K. Ozdemir, J. Zhu, W. Kim, and L. Yang, "Detecting single viruses and nanoparticles using whispering gallery microlasers," Nat. Nano. **6**, 428-432 (2011).
4. J. Zhu, S. K. Ozdemir, Y.-F. Xiao, L. Li, L. He, D.-R. Chen, and L. Yang, "On-chip single nanoparticle detection and sizing by mode splitting in an ultrahigh-Q microresonator," Nat. Photon. **4**, 46-49 (2010).
5. J. Wang, T. Zhan, G. Huang, P. K. Chu, and Y. Mei, "Optical microcavities with tubular geometry: properties and applications," Las. Phot. Rev. **8**, 521-547 (2014).
6. C. M. Hessel, M. A. Summers, A. Meldrum, M. Malac, and J. G. C. Veinot, "Direct patterning, conformal coating, and erbium doping of luminescent nc-Si/SiO2 thin films from solution processable hydrogen silsesquioxane," Adv. Mater. **19**, 3513-3516 (2007).
7. P. Bianucci, J. R. Rodríguez, F. C. Lenz, J. G. C. Veinot, and A. Meldrum, "Mode structure in the luminescence of Si-nc in cylindrical microcavities," Physica E Low Dimens. Syst. Nanostruct. **41**, 1107-1110 (2009).
8. I. White, H. Zhu, J. Suter, X. Fan, and M. Zourob, "Label-free detection with the liquid core optical ring resonator sensing platform," in *Biosensors and Biodetection*, A. Rasooly, and K. Herold, eds. (Humana, 2009), pp. 139-165.
9. C. P. K. Manchee, V. Zamora, J. W. Silverstone, J. G. C. Veinot, and A. Meldrum, "Refractometric sensing with fluorescent-core microcapillaries," Opt. Express **19**, 21540-21551 (2011).
10. M. R. Foreman, J. D. Swaim, and F. Vollmer, "Whispering gallery mode sensors," Adv. Opt. Photon. **7**, 168-240 (2015).

11. M. D. Baaske, M. R. Foreman, and F. Vollmer, "Single-molecule nucleic acid interactions monitored on a label-free microcavity biosensor platform," Nat. Nanotechnol. **9**, 933-939 (2014).
12. G. Zhixiong, Q. Haiyong, and P. Stanley, "Near-field gap effects on small microcavity whispering-gallery mode resonators," J. Phys. D Appl. Phys. **39**, 5133-5136 (2006).
13. Y. Zhi, J. Valenta, and A. Meldrum, "Structure of whispering gallery mode spectrum of microspheres coated with fluorescent silicon quantum dots," JOSA B **30**, 3079-3085 (2013).
14. N. Riesen, T. Reynolds, A. François, M. R. Henderson, and T. M. Monro, "Q-factor limits for far-field detection of whispering gallery modes in active microspheres," Opt. Express **23**, 28896-28904 (2015).
15. A. François, T. Reynolds, and T. Monro,"A fiber-tip label-free biological sensing platform: A practical approach toward in-vivo sensing," Sensors **15**, 1168-1181 (2015).
16. G. S. Huang, V. A. B. Quinones, F. Ding, S. Kiravittaya, Y. F. Mei, and O. G. Schmidt, "Rolled-up optical microcavities with subwavelength wall thicknesses for enhanced liquid sensing applications," ACS Nano. **4**, 3123-3130 (2010).
17. S. Lane, J. Chan, T. Thiessen, and A. Meldrum, "Whispering gallery mode structure and refractometric sensitivity of fluorescent capillary-type sensors," Sensor Actuat. B-Chem. **190**, 752-759 (2014).
18. K. J. Rowland, A. François, P. Hoffmann, and T. M. Monro, "Fluorescent polymer coated capillaries as optofluidic refractometric sensors," Opt. Express **21**, 11492-11505 (2013).
19. V. Zamora, Z. Zhang, and A. Meldrum, "Refractometric sensing of heavy oils in fluorescent core microcapillaries," Oil Gas Sci. Technol. – Rev. IFP Energies Nouvelles **70**, 487-495 (2013).
20. R. Arshady, "Microspheres for biomedical applications - preparation of reactive and labeled microspheres," Biomaterials **14**, 5-15 (1993).
21. K. J. Rowland, A. François, P. Hoffmann, and T. M. Monro, "Fluorescent polymer coated capillaries as optofluidic refractometric sensors," Opt. Express **21**, 11492-11505 (2013).
22. S. Lane, P. West, A. François, and A. Meldrum, "Protein biosensing with fluorescent microcapillaries," Opt. Express **23**, 2577-2590 (2015).
23. Y. Jun, and L. J. Guo, "Optical sensors based on active microcavities," IEEE J. Sel. Top. Quantum Electron. **12**, 143-147 (2006).
24. J. C. Knight, H. S. T. Driver, R. J. Hutcheon, and G. N. Robertson, "Core-resonance capillary-fiber whispering-gallery-mode laser," Opt. Lett. **17**, 1280-1282 (1992).
25. P. Li, C. Xu, M. Jiang, J. Dai, J. Li, and J. Lu, "Lasing behavior modulation in a layered cylindrical microcavity," Appl. Phys. B **118**, 93-100 (2015).
26. H.-J. Moon, Y.-T. Chough, J. B. Kim, K. An, J. Yi, and J. Lee, "Cavity-Q-driven spectral shift in a cylindrical whispering-gallery-mode microcavity laser," Appl. Phys. Lett. **76**, 3679-3681 (2000).
27. H.-J. Moon, Y.-T. Chough, and K. An, "Cylindrical microcavity laser based on the evanescent-wave-coupled gain," Phys. Rev. Lett. **85**, 3161-3164 (2000).
28. H. Yanagi, R. Takeaki, S. Tomita, A. Ishizumi, F. Sasaki, K. Yamashita, and K. Oe, "Dye-doped polymer microring laser coupled with stimulated resonant Raman scattering," Appl. Phys. Lett. **95**, 033306 (2009).
29. Y. Yoshida, T. Nishimura, A. Fujii, M. Ozaki, and K. Yoshino, "Dual ring laser emission of conducting polymers in microcapillary structures," Appl. Phys. Lett. **86**, 141903 (2005).
30. Y. Yuichi, N. Tetsuharu, F. Akihiko, O. Masanori, and Y. Katsumi, "Lasing of Poly(3-alkylthiophene) in microcapillary geometry," Jpn. J. Appl. Phys. **44**, L1056-L1058 (2005).
31. A. François, N. Riesen, H. Ji, S. Afshar V., and T. M. Monro, "Polymer based whispering gallery mode laser for biosensing applications," Appl. Phys. Lett. **106**, 031104 (2015).
32. M. Akbulut, P. Ginart, M. E. Gindy, C. Theriault, K. H. Chin, W. Soboyejo, and R. K. Prud'homme, "Generic method of preparing multifunctional fluorescent nanoparticles using flash nanoprecipitation," Adv. Funct. Mater. **19**, 718-725 (2009).
33. C.-Y. Tan and Y.-X. Huang, "Dependence of refractive index on concentration and temperature in electrolyte solution, polar solution, nonpolar solution, and protein solution," J. Chem. Eng. Data **60**, 2827-2833 (2015).
34. Poly(benzyl methacrylate) (Polysciences, 2015), http://www.polysciences.com/default/catalog-products/polybenzyl-methacrylate/
35. A. Meldrum and F. Marsiglio, "Capillary-type microfluidic sensors based on optical whispering gallery mode resonances," Rev. Nanosci. Nanotechnol. **3**, 193-209 (2014).
36. I. Teraoka and S. Arnold, "Enhancing the sensitivity of a whispering-gallery mode microsphere sensor by a high-refractive-index surface layer," J. Opt. Soc. Am. B **23**, 1434-1441 (2006).
37. G. M. Hale and M. R. Querry, "Optical constants of water in the 200-nm to 200-μm wavelength region," Appl. Optics **12**, 555-563 (1973).
38. I. H. Malitson, "Interspecimen comparison of the refractive index of fused silica," J. Opt. Soc. Am. **55**, 1205-1209 (1965).
39. Z. Zhang, P. Zhao, P. Lin, and F. Sun, "Thermo-optic coefficients of polymers for optical waveguide applications," Polymer **47**, 4893-4896 (2006).
40. I. M. White and X. Fan, "On the performance quantification of resonant refractive index sensors," Opt. Express **16**, 1020-1028 (2008).
41. J. W. Silverstone, S. McFarlane, C. P. K. Manchee, and A. Meldrum, "Ultimate resolution for refractometric sensing with whispering gallery mode microcavities," Opt. Express **20**, 8284-8295 (2012).

42. S. Berneschi, D. Farnesi, F. Cosi, G. N. Conti, S. Pelli, G. C. Righini, and S. Soria, "High Q silica microbubble resonators fabricated by arc discharge," Opt. Lett. **36**, 3521-3523 (2011).
43. H. Li, and X. Fan, "Characterization of sensing capability of optofluidic ring resonator biosensors," Appl. Phys. Lett. **97**, 011105 (2010).

1. Introduction

Whispering gallery modes (WGMs) are resonances that occur when light is trapped by total internal reflection (TIR) within a structure presenting at least one axis of revolution. Common WGM resonators include spheres [1, 2], disks and toroids [3, 4], optical fibers [5-7], and capillaries [8, 9]. WGM resonators have attracted considerable interest within the sensing community largely due to their potential use in refractometry-based fluid sensing and label-free biosensing applications [10]. While there are many examples of remarkable sensing performance using such optical resonators [3, 4, 11], the interogation strategies typically used are cumbersome and impractical. The typical approach involving evanescent coupling to excite and probe the WGMs, relies on the use of a tapered optical fiber or prism that is phase-matched to the resonator. In such a setup the coupling efficiency is however never perfectly stable, and the coupler can cause undesired resonance wavelength shifts or Q-spoiling due to slight movements and vibrations [12].

In contrast, fluorescence-based resonators do not have the same practical limitations. Rather than using a waveguide or prism to evanescently couple light into and out of the device, a fluorophore is used to excite the resonances indirectly. This permits remote excitation and detection of a WGM-modulated fluorescence spectrum. The performance of fluorescence-based microresonators is, however, in general far worse than for their passive counterparts. This is due in part to the significantly lower achievable Q factors resulting from absorption, scattering, and the intrinsically broad linewidth of the emitters [13], as well as intrinsic resonator asphericity [14]. One particular strategy that can improve the performance is to induce lasing of the WGMs. It has been shown previously that lasing of the WGMs in dye-doped microspheres enables a two fold increase in Q factor, resulting in improved detection limits for refractive index sensing compared with microspheres operated below the lasing threshold [15].

Among the different resonator geometries supporting WGMs, capillaries have the unique property of having the evanescent fields extend into and sample the medium *inside* the resonator, which is particularly interesting because the resonator itself serves as a microfluidic channel. Fluorescent capillary resonators have previously been demonstrated [9, 16-19], in essence building on the considerable body of literature on fluorescent microspheres going back many years [20]. In this context, the gain medium can be introduced through a thin high-refractive-index coating deposited onto the inner surface of the capillary. Examples of such coatings include dye-doped polymers [21] and semiconductor quantum dots [22]. The resonator itself then provides the optofluidic channel through which a liquid solution can be delivered and sampled simultaneously.

Previously, lasing has been exploited in microspheres to decrease the resonance linewidths (i.e. increase the Q factors) and therefore improve the detection limit [23], or to enable alternative sensing modalities involving for instance mode-splitting for the detection of nanoparticles [3]. The first demonstration of any type of lasing WGMs in capillaries was performed by Knight *et al.* [24], in which a thin-walled capillary was simply filled with a rhodamine 6G solution. Subsequently several variations of the same concept were reported [25-27], although filling the entire capillary with a gain medium is not readily compatible with the main purpose of using these structures as optofluidic refractive index sensors. Although lasing has previously been shown in high refractive index polymer coated capillaries [28-30], these demonstrations have been restricted to the use of very high refractive index polymer (n>1.67)

and thick polymer coatings (1.9 µm) [28], making these lasing microcapillaries unsuitable for refractive index sensing applications.

Here we investigate the lasing behavior of optofluidic capillary resonators and their application to refractive index sensing. We demonstrate the first channel-coated lasing microcapillary suitable for refractive index sensing and investigate the conditions under which lasing occurs. We analyze the refractometric sensing capacity of these devices below and above the lasing threshold, determining whether lasing provides a significant benefit to the overall performance.

2. Materials and methods

2.1 Preparation of active optofluidic resonators

Commercial silica capillaries (Beckman Coulter) with inner and outer diameters of 50 and 360 µm, respectively, were processed as follows. First the polyimide coating was removed from the outer surface of the capillary using a blowtorch and the residue was wiped off with ethanol. Different solutions of poly (benzyl methacrylate) (PBZMA; Polysciences) in tetrahydrofuran (THF) were then prepared with various concentrations (25, 50, 75 and 100 mg/mL) for coating the inner surface of the capillary. Another solution was also prepared, consisting of a fluorescent dye (Nile Red) dissolved in THF up to its solubility limit. The dye was the gain medium to be doped within the deposited polymer coating. This particular organic dye was chosen for its excellent lasing properties [31] and convenient emission spectrum between 590 and 630 nm. Subsequently, 200 µL of each polymer solution was combined with 10 µL of the gain medium solution, and each resulting mixture was allowed to fill a capillary by capillary forces.

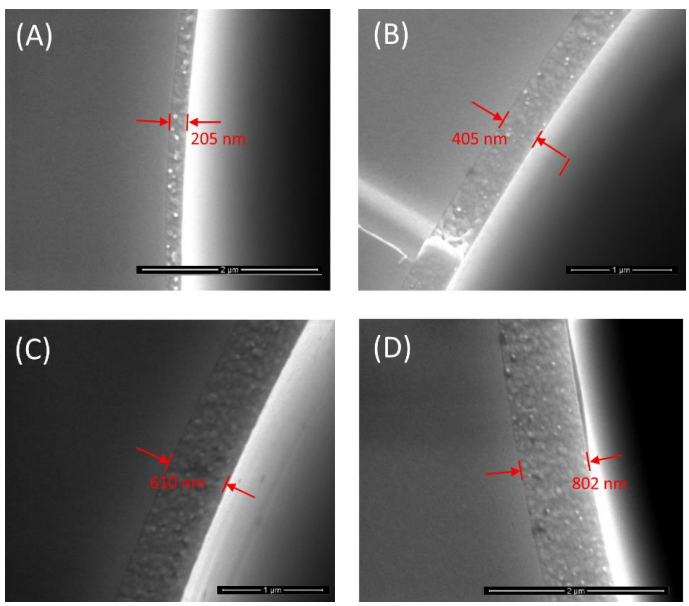

Fig. 1. Cross-sectional SEM images (90,000 times magnification) of the polymer coated capillaries for polymer solution concentrations of (A) 25, (B) 50, (C) 75 and (D) 100 mg/mL.

Once the capillaries were filled with the fluorescent polymer solutions described above, they were placed in an oven at 70°C for 1 h, allowing the solvent to evaporate. During this process, as the solvent evaporates the meniscus leaves behind a thin layer of polymer on the

channel surface as it retreats down the length of the capillary [21]. The thickness *t* of the resulting polymer layer was then measured by cleaving several sections of the given polymer coated capillary and examining them end-on using a field emission scanning electron microscope (FEI Quanta 450 FEG, 10 kV) in the secondary electron mode. Figure 1 shows typical SEM images for the four different polymer coated capillaries. The SEM images permit the characterization of the relationship between thickness of the deposited polymer coating and the polymer solution concentration (Table 1). There was excellent controllability, with a near-linear relationship between polymer solution concentration and coating thickness. The uniformity of the layer along the length of the capillary was however impossible to assess due to the enclosed nature of the resonator.

Once the relationship between the polymer solution concentration and the resulting thickness of the deposited layer was established, a new batch of capillaries was prepared but this time adjusting the amount of dye in each sample to ensure it matches the optimum lasing concentration of 5 µg/mL [32]. This concentration enables one to reach the maximum gain of the fluorescent dye, thereby reducing the lasing power threshold. Increasing the dye concentration beyond this point results in self-quenching due to non-radiative energy transfer between nearby dye molecules [32].

2.2 Optical setup

The optical setup shown in Fig. 2 was used for measuring the WGM spectra of the dye-doped polymer coated capillaries. The excitation of the WGMs was achieved using either a 532 nm CW laser (JDS Uniphase), or, for the case of characterizing the lasing behavior, a 532 nm frequency doubled Nd:YAG laser (Quanta-Ray INDI, Spectra Physics, 10 Hz, 5 ns pulses). Neutral density filters were used to adjust the excitation power in the latter case, while an energy meter (Gentec-E0 M link) was used for measuring the absolute pulse energy delivered to the capillary. A 10× microscope objective was used for focusing the laser (spot size ~ 400 µm in diameter) onto the capillary, which was mounted onto a 3-axis translation stage (Thorlabs NanoMax). A second microscope objective (20×) was used to collect the WGM-modulated fluorescence signal from the capillaries. A longpass filter (λ = 550 nm) was used to remove the scattered pump laser light, and an analyzer was used for selecting the WGM polarization. Here the TE polarization (electric field parallel to the capillary axis) was selected to increase mode visibility, since the TE modes tend to exhibit higher Q factors compared with the TM modes, and hence also have lower lasing thresholds [31]. We note however that the refractive index sensitivity of the TE modes is marginally smaller compared with the TM modes [17].

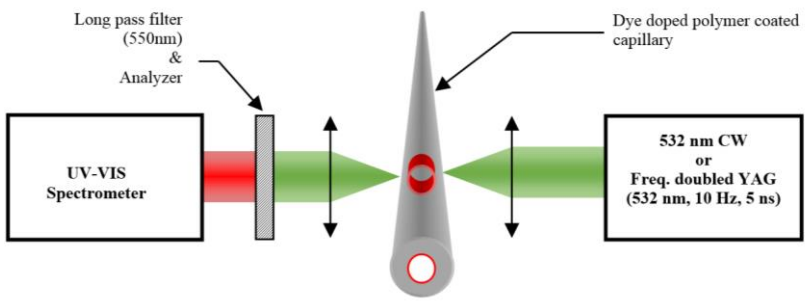

Fig. 2. Depiction of the optical setup used for measuring the WGM-modulated fluorescence spectra from the dye-doped polymer coated capillaries.

The fluorescence signal was spectrally resolved using a UV-VIS spectrometer (Horiba iHR 550) equipped with a 1200 lines/mm grating and a 2048-pixel CCD camera (Horiba Synapse). This system has a nominal spectral resolution of 18 pm. One end of the capillary was then

connected to a syringe pump, allowing liquids with different refractive indices to be pumped through the capillary for refractometric measurements. The solutions used were different concentrations of glucose in water, since this system is simple to work with and the refractive index as a function of concentration is well known [33]. Fluid that flowed out of the ejection end of the capillary was simply allowed to collect inside a small container.

2.3. Optical constants of PBZMA

The refractive index of PBZMA is nominally 1.568 at a wavelength of 589.3 nm [34]. Polymers can, however, have significant dispersion across the broad gain bands associated with fluorescent dyes. Since no data is available in the literature for the wavelength-dependence of the optical constants of PBZMA, they had to be measured using variable angle spectroscopic ellipsometry (VASE). First, a polymer film was fabricated by spin coating PBZMA in either toluene or tetrahydrofuran (THF) at a rate of 6100 rev/minute onto a standard silicon wafer. The reflection spectra were measured on a JA Wollam model M-2000V spectroscopic ellipsometer, and the measured ellipsometric ψ and Δ values (relating to the reflected amplitude and phase) were least-squares fit using a standard Fresnel model to extract the optical constants, Cauchy coefficients, and the thickness of the polymer. The PBZMA films deposited from toluene were found to be smooth over large areas, as inferred from the uniformity of the film interference colors over a range of ~1 cm^2, whereas those deposited from THF had observable surface ripples on a millimeter scale. The smoother polymer film yielded smaller uncertainties in the values of the Cauchy coefficients in the model fit.

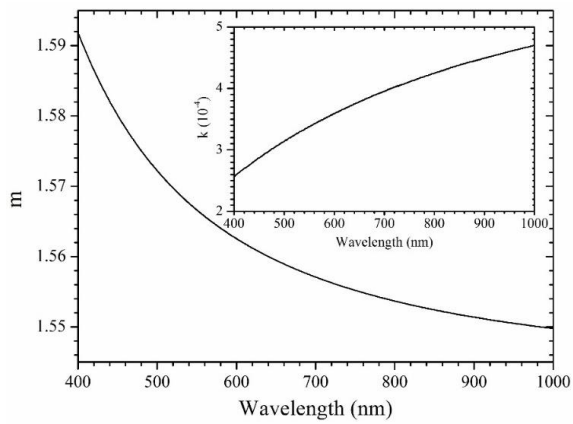

Fig. 3. Optical constants of the PBZMA film. The main panel shows the real part of the refractive index (*m*) and the inset shows the extinction coefficient (κ).

The resulting optical constants for the polymer film are shown in Fig. 3, with the coefficients of the Cauchy model $m(\lambda) = A + B/\lambda^2 + C/\lambda^4$ found to be $A = 1.5420 \pm 0.0003$, $B = 0.00628 \pm 0.00003$ and $C = 0.000240 \pm 0.000004$, where m is the refractive index. The refractive index obtained at the reference wavelength of $\lambda = 589.3$ nm was found to be slightly lower than the one quoted by the manufacturer (1.563 vs. 1.568, respectively) [34].

3. Results and discussion

3.1. Whispering gallery mode structure

To model the whispering gallery modes of the coated capillaries, estimate the Q factor and refractometric sensitivity, and to verify experimental observations, the electric field profiles of the modes were first modeled following the method described in Ref. [35], which is based on an earlier theory for spherical resonators [36]. Accordingly, the refractive index profile of the coated capillary is,

$$m(r)=\begin{Bmatrix} m_1, & r\le b \\ m_2, & b<r\le a \\ m_3, & r>a \end{Bmatrix}, \tag{1}$$

where m_1, m_2 and m_3 are the refractive indices in the channel, polymer layer and capillary wall, respectively, whilst a and b are the outer and inner radii of the polymer coating of thickness $t = a - b$. By applying the relevant boundary conditions for the cylindrical harmonics associated with the TE polarization, the radial electric field function is given by [35],

$$E_S\left(m_1k_0r\right)=\begin{Bmatrix} A_lJ_1\left(m_1k_0r\right), & r\le b \\ B_lH_l^{(2)}\left(m_1k_0r\right)+C_lH_l^{(1)}\left(m_2k_0r\right), & b<r\le a \\ D_lH_l^{(1)}\left(m_3k_0r\right) & r>a \end{Bmatrix}, \tag{2}$$

with azimuthal mode number l and arbitrary coefficients A_l, B_l, C_l and D_l, with C_l set to unity. In Eq. (2), the definitions are as usual: $J_l(R)$ is the cylindrical Bessel function of the first kind and $H_l^{(1,2)}(R)$ are the cylindrical Hankel functions given by $H_l^{(1)}(R) = J_l(R) + iY_l(R)$ and $H_l^{(2)}(R) = J_l(R) - iY_l(R)$, respectively, with $Y_l(R)$ being the cylindrical Bessel function of the second kind and the argument $R = mk_0r$. The relative field intensity is found by setting I proportional to $|E_S|^2$. Setting the electric field and its derivatives equal at the boundaries as appropriate for the TE polarization (E field parallel to cylinder axis) one obtains,

$$\frac{m_3H_l^{(1)'}\left(m_3k_0a\right)}{m_2H_l^{(1)}\left(m_3k_0a\right)}=\frac{B_lH_l^{(2)'}\left(m_2k_0a\right)+H_l^{(1)'}\left(m_2k_0a\right)}{B_lH_l^{(2)}\left(m_2k_0a\right)+H_l^{(1)}\left(m_2k_0a\right)}, \tag{3}$$

where,

$$B_l=\frac{m_2J_1\left(m_1k_0b\right)H_l^{(1)'}\left(m_2k_0b\right)-m_1J_l^{'}\left(m_1k_0b\right)H_l^{(1)}\left(m_2k_0b\right)}{-m_2J_1\left(m_1k_0b\right)H_l^{(2)'}\left(m_2k_0b\right)+m_1J_l^{'}\left(m_1k_0b\right)H_l^{(2)}\left(m_2k_0b\right)}, \tag{4}$$

By numerically solving Eqs. (3) and (4) for the complex roots k_0, the quality factor is then simply $Q = \mathrm{Re}[k_0]/2\mathrm{Im}[k_0]$ and the resonance wavelength is $\lambda_0 = 2\pi/\mathrm{Re}[k_0]$. The electric field intensity profiles are calculated by first solving for the constants A_l and D_l that satisfy the continuous boundary conditions for the TE polarization. The results are shown in Fig. 4 for 800, 600, 400 and 200 nm polymer coatings. Each of the intensity profiles shown is for the resonance closest to 610 nm, in accordance with the experimental results in Fig. 5. Finally, the refractive index sensitivity of the capillary channel is given by,

$$S_{TE}=\frac{\lambda_0}{m_1}\frac{I_1}{I_1+I_2+I_3}, \tag{5}$$

in which I_1, I_2, and I_3 are the relative field intensities in the channel, polymer layer, and capillary wall, respectively. These values can be obtained by substituting k_0 into the three piecewise parts of Eq. (2) and squaring the result. As shown later in Table 1, the Q factors computed using this model agree reasonably closely with the experimental results for the non-lasing capillaries.

Moreover, the free spectral ranges predicted by Eqs. (1-5) are found to be virtually identical to the measured values.

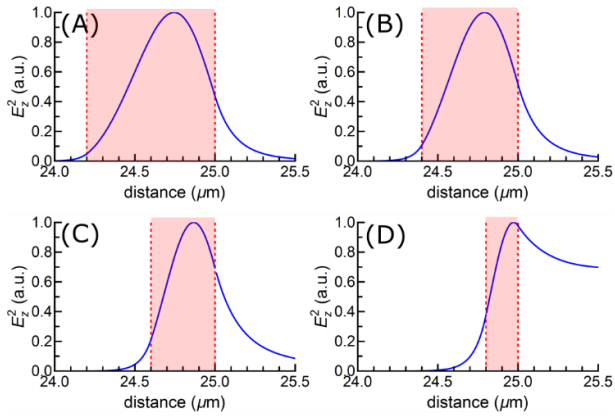

Fig. 4. Intensity profiles for the resonance closest to 610 nm (i.e. l = 390–377) for polymer thicknesses: (A) 800 nm, (B) 600 nm, (C) 400 nm and (D) 200 nm. The thin polymer film is represented by the red-shaded region between the dotted lines; the inner region is water [37] and the outer region is silica glass [38]. Dispersion was incorporated for all calculations.

3.2 WGMs in polymer coated capillaries

The capillaries were then filled with millipore water using the connected syringe pump and the fluorescent WGMs for each capillary were excited with the 532 nm CW laser as pump source (~1 mW, 0.1s acquisition). Typical WGM spectra for the capillaries with different coating thicknesses are shown in Fig. 5.

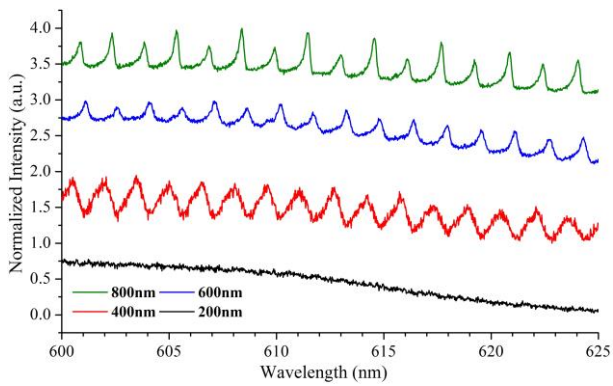

Fig. 5. WGM spectra of the dye-doped polymer coated capillaries with the polymer coating thickness varying from 200-800 nm. For clarity the different spectra were normalized and offset.

The thinnest coating (200 nm) exhibited only background fluorescence and no modes were observed, although the numerical calculation of the electric field shown in Fig. 4 (D) predicts the existence of very low-Q WGMs. At a polymer thickness of 400 nm, the modes were clearly visible (Q ~ 460) despite the considerable background noise. The WGM signal-to-noise ratio and Q factor increased further for the 600 and 800 nm polymer layer thicknesses. For the 800 nm polymer coating a Q factor as high as ~2800 was observed. Additionally, a periodic modulation of the WGM spectrum was apparent for the thicker films, in which every second

mode was distinctly more intense. This effect probably arises from interference associated with reflections coming from the outer walls of the capillary [24].

3.3. Lasing WGMs in coated capillaries

The lasing capability of the capillaries supporting WGMs was investigated by replacing the CW pump laser with the frequency doubled Nd:YAG laser. The WGM spectra of the different capillaries were then acquired as a function of the incident pulse energy. Figs. 6 (A)-(C) show the typical behavior observed as the pump energy is increased. As reported for other fluorescent resonators, such as microspheres [31], a clear transition or threshold exists upon which some modes start lasing. The fluorescence intensity of the resonance modes and their Q factors, exhibit two different regimes depending on the pulse energy; *i.e.* the fluorescence regime and the stimulated emission regime, as shown in Fig. 6 (D). For the various capillaries tested, only those with a polymer coating thickness of 600 or 800 nm exhibited this lasing behavior, with lasing thresholds of 16 ± 2 μJ and 1.2 ± 0.1 μJ, respectively. The large error on the lasing threshold is predominately due to the fluctuation of the laser pulse energy (± 11%).

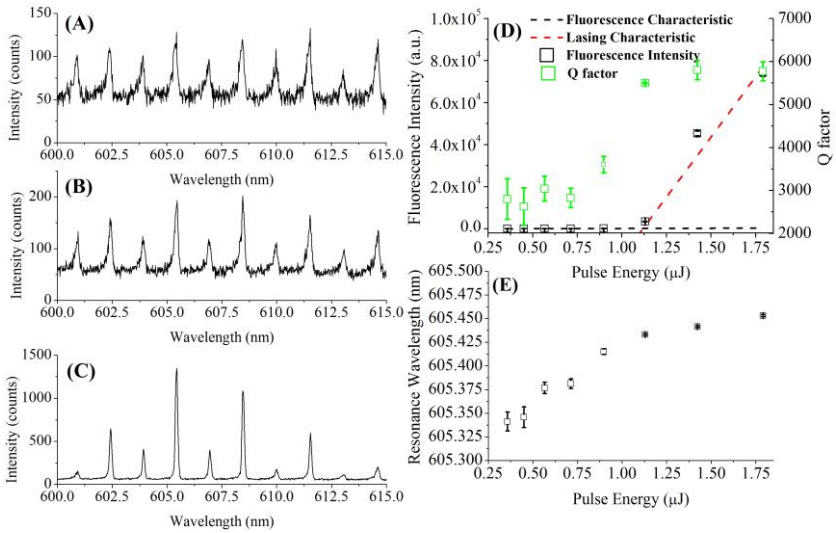

Fig. 6. (A), (B) and (C) WGM spectrum of the capillary with the 800 nm thick polymer coating, for pump powers of 0.71, 0,89 and 1.13 μJ respectively. (D) The intensity of the dominant resonance (black symbols) and its Q factor (green symbols) as a function of the pulse energy. The dashed lines highlight both the fluorescence (black) and stimulated emission regimes (red). (E) The fluctuation of the resonance position as a function of the pump pulse energy for the most intense resonance.

For both of the lasing capillaries, significant increases in the Q factor were observed upon transitioning into the lasing regime. The 600 nm thick polymer coated capillaries exhibited a Q factor of 1800 below and 4000 above the lasing threshold, while those with the 800 nm coating exhibited a Q factor of 2800 below and 6000 above the lasing threshold. In both cases the increase in Q factor was by approximately a factor of 2, which is comparable to values for lasing WGMs in dye-doped microspheres [31]. Surprisingly, the resonance position was also found to vary with the pump energy as seen in Fig. 6 (E), although this behavior hasn't been reported for other polymer-based WGM lasers (the vast majority being made of polystyrene). Whereas the thermo-optic constants for polystyrene can be found in the literature [39], the values are not available for PBZMA. Thus, whilst an intensity-induced redshift is probably

consistent with heating effects in the polymer, capillary, and channel region, the lack of any data on PBZMA renders difficult an unambiguous interpretation of this phenomenon. This behavior highlights the need to keep the pump energy constant to avoid any drift in the resonance position for refractive index sensing applications.

3.4. Refractive index sensing with lasing and non-lasing capillaries

Refractive index sensing measurements were performed with both the 800 nm thick polymer coated lasing capillary and the 400 nm polymer coated non-lasing capillary. Although the 600 nm polymer coated capillary also exhibited lasing behavior, it proved impossible to sustain the lasing operation over the timeframe required for completing the refractive index sensing measurements due to rapid photobleaching of the gain medium at the higher pump power required. Increasing the pump energy was avoided as this affects the resonance wavelength as previously stated. Therefore we limited the refractive index sensing measurements to the following two scenarios; (i) using the non-lasing capillary with presumably the highest refractive index sensitivity (i.e. 400 nm thick polymer coating) and (ii) the capillary with the highest Q factor and also stable lasing operation (i.e. 800 nm thick polymer coating).

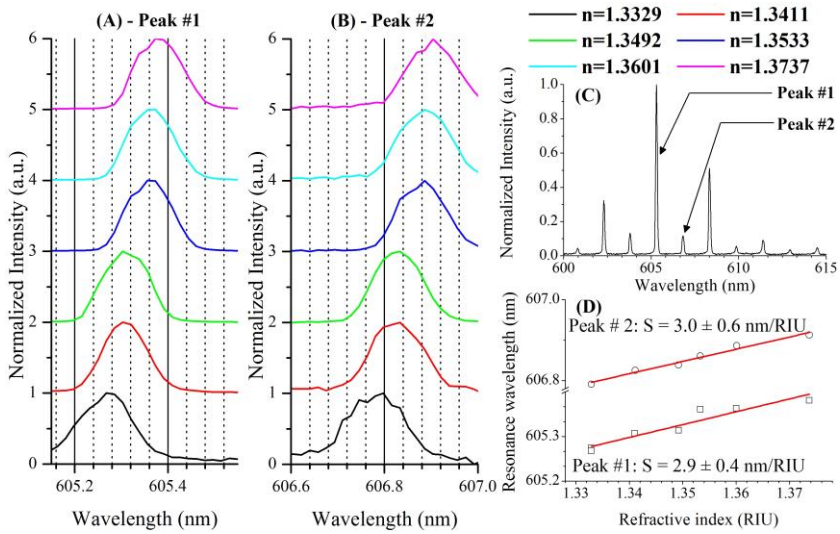

Fig. 7. (A)-(B) Two lasing WGM resonances of the 800 nm polymer coated capillary, monitored as different refractive index solutions were pumped through the channel. (C) The entire lasing WGM spectrum of the same capillary showing the two monitored resonances and (D) the resonance positions as a function of the refractive index inside the capillary channel.

To measure the refractometric sensitivity, different concentration solutions of glucose in water were pumped into each capillary. The typical behavior of two consecutive first order resonances (see complete spectrum in Fig. 7 (C)) of the lasing capillary with 800 nm thick polymer coating is demonstrated in Figs. 7 (A) and 7 (B), as the concentration of glucose increases. The central positions of the resonances were calculated by fitting them with Lorentzian functions. The resonance positions are shown in Fig. 7 (D) as a function of the refractive index of the fluid inside the capillary. Under these conditions, a refractive index sensitivity of 2.9 ± 0.4 nm/RIU was measured with the lasing capillaries for the most intense peak, and the second mode considered with lower intensity (e.g. Fig. 7 (B)) exhibited similar sensitivity (3.0 ± 0.6 nm/RIU). The sensitivities were also measured below the lasing thresholds and were found to be within the errors stated above. The non-lasing capillary (400 nm polymer

coating) tested under the same conditions had a refractive index sensitivity of 23.0 ± 0.8 nm/RIU. Note that the experimental results consistently have a factor 2 higher sensitivity compared to the predicted values. While the origin of this discrepancy remains uncertain, it has been observed before in non-lasing fluorescent capillaries [17], in which it was tentatively attributed to interference effects caused by reflection of a portion of the emitted fluorescence at the external interface. Alternatively, a fluctuation of the polymer coating thickness inside the capillary, which is however inherently difficult to measure, could be partially responsible for the higher-than-expected refractive index sensitivities [21].

Table 1. Thickness of the polymer coating, and the Q factor of the WGMs as a function of polymer concentration.

Polymer Concentration (mg/mL)	Polymer Thickness (Mean ± Stand. Dev.)	Lasing Threshold (μJ)	Q factor Below and *Above* Lasing Threshold (Exp.)	Q factor (Theory)	S nm/RIU (Exp.)	S nm/RIU (Theory)
100	799 ± 16	1.2 ± 0.1	2800 *6000*	2170	3.0	1.7
75	590 ± 25	16 ± 2	1800 *4000*	1920	-	4.3
50	414 ± 14	NA	460 *NA*	784	23	10.2
25	211 ± 13	NA	NA	75	NA	19.0

It becomes apparent that there is a tradeoff in achieving lasing in optofluidic capillaries. A thicker polymer coating is required to sustain the high Q factors necessary to achieve lasing and to also minimize photobleaching by ensuring a low lasing threshold. The thicker polymer coating however reduces the refractive index sensitivity. The sensitivity by itself can however be a rather misleading parameter for evaluating the performance of a given resonator [40]. The detection limit (DL) which represents the smallest refractive index change that is measurable is more relevant [40]. The detection limit of the resonator is given by the ratio of the sensor resolution (R) and the resonator sensitivity (S), DL = R/S [40]. Several formalisms have been developed for calculating the (wavelength shift) resolution, R. For example, White *et al.* [40] calculate the resolution based on the accuracy which resonance maxima can be determined, whereas Silverstone *et al.* [41] base the resolution on model fits and Fourier analysis.

Using the approach given by White *et al.* [40], the sensor resolution is 3σ of the noise in the system and can be approximated by,

$$3\sigma = 3\sqrt{\sigma_{amp}^2 + \sigma_{temp}^2 + \sigma_{spect}^2}, \tag{6}$$

where σ_{amp} is amplitude noise, σ_{temp} is temperature induced noise, and σ_{spect} is spectrometer noise associated with the finite spectral resolution of the spectrometer. The amplitude noise (σ_{amp}) relates to the Q factor and the signal-to-noise ratio (SNR) of the resonances, and can be approximated as,

$$\sigma_{amp} \approx \frac{1}{4.5}\frac{\lambda}{(SNR)^{1/4} Q}, \tag{7}$$

where λ is the resonance wavelength and the SNR is in linear units. This term accounts for the uncertainty in the location of the resonance peak. Here we assume the conservative values of 10 fm for the temperature induced noise (σ_{temp}) and 0.29 pm for the spectral noise (σ_{spect}) given by White *et al.* [40]. We find that the 800 nm polymer coated lasing capillaries (SNR = 50 dB) have an approximately 127 times higher wavelength shift resolution than the 400 nm polymer coated non-lasing capillaries (SNR = 10 dB). The refractive index sensitivity of the lasing capillary is however 8 times lower than for the non-lasing capillary. Despite this the detection

limit is actually an order of magnitude greater (i.e. a 13-fold increase) for the lasing capillary (1.2×10^{-3} RIU and 1.6×10^{-2} RIU for the 800 nm lasing and 400 nm non-lasing capillaries respectively).

Alternatively, using the formalism by Silverstone *et al.* [41], the wavelength shift resolution is given by,

$$\Delta\lambda_{min} = \frac{2.2\times10^{-20}\times\Delta f_{peak}^{0.29}\times P^{0.65}}{SNR^{0.51}}, \tag{8}$$

where Δf_{peak} is the full width at half maximum of the resonance and P is the pitch of the spectrometer (i.e. the spectral frequency range per pixel), both in Hz. Given a Q factor enhancement of a factor 2 and a signal-to-noise ratio (SNR) increase from ~10 to 50 dB, as observed here, the minimum wavelength shift measurable can decrease significantly. Taking into account the improvement in the wavelength shift resolution of the lasing capillaries from Eq. (8) and factoring in the lower sensitivity, one obtains an overall detection limit 16 times smaller compared with the non-lasing capillaries. Both formalisms for calculating the wavelength shift resolution therefore suggest significantly improved detection limits for the lasing capillary by around an order of magnitude. The increase in the wavelength shift resolution overwhelms the decreased sensitivity imposed by the necessity to use thicker polymer coatings to achieve stable lasing in the lasing microcapillaries.

4. Conclusion

In this paper we demonstrated for the first time lasing of the whispering gallery modes in polymer coated optofluidic capillaries for refractive index sensing. The lasing operation requires the introduction of a gain medium such as Nile Red dye into the high-refractive-index polymer coating. The coating also has to be of sufficient thickness to support modes with high Q factors that permit low-enough lasing thresholds to avoid the issue of photobleaching. The refractive index sensitivities of optofluidic resonators with different polymer coating thicknesses were characterized, revealing that high Q factor lasing capillaries (requiring thicker coatings) exhibit significantly lower refractive index sensitivities. However, the detection limit, given by the ratio of sensor resolution and sensitivity, improves significantly upon lasing. This is mainly because of the dramatic increase in signal-to-noise ratio and Q factor when the sensors are pumped above their lasing thresholds. While other hollow resonators, such as microcapillaries and microbubbles, have been used for refractive index sensing with even lower detection limits [42, 43], our platform does not require the use of a fiber taper for probing the WGM resonances. Instead our approach relies on the gain medium inside the resonator for free space excitation and collection of the WGMs, making the setup simpler to use and implement. Further improvements could be made to the sensing properties, by using a more efficient gain medium which would allow for a reduction in the lasing threshold or a reduction in Q factor requirements. The latter would make it possible to achieve lasing with thinner polymer coatings. Inducing lasing in a 400 nm thick polymer coating, would for example allow for a detection limit in the range of 10^{-5} RIU to be reached.

Acknowledgments

The authors acknowledge the support of T. M. M's ARC Georgina Sweet Laureate Fellowship, and a University of Adelaide Priority Partner Grant. The authors also thank Dr. Georgios Tsiminis for his technical support and Dr. Kristopher J. Rowland for his advice. NSERC and and AITF provided support for this work.